Surface states of a semi-infinite superlattice

Walter L. Bloss
Electronics Technology Center, The Aerospace Corporation, P. O. Box 92957, Los Angeles, California 90009
(Received 15 May 1991)

The surface states of a semi-infinite superlattice with a step discontinuity in the potential at the interface has been calculated within the framework of the Kronig-Penney model. An explicit solution is obtained for the eigenenergy of the surface state. Surface states are shown to exist only for certain values of the barrier widths and/or heights of the semi-infinite superlattice and of the potential step discontinuity at the interface. Approximate, but very accurate, formulas are derived for the surface-state energy and its respective characteristic decay length, allowing one to readily determine the conditions for the existence of surface states.

I. INTRODUCTION

There has been a substantial research effort in the physics of quantum-well structures stemming from the recent developments in the crystal-growth techniques exemplified by molecular-beam epitaxy (MBE) and metalorganochemical vapor deposition (MOCVD). With these precise crystal-growth methods, one can now grow high-quality structures with tailored band-gap profiles and with a multitude of layers with thicknesses ranging from a single monolayer to hundreds of angstroms. Structures and phenomena, involving quantum confinement, reduced dimensionality, and superlattices, have been predicted and experimentally observed. Recently, there has been interest in the surface states of a semi-infinite superlattice with a step discontinuity at the interface. These type structures are easily grown by MBE or MOCVD and provide an excellent experimental vehicle to study the early predictions of Tamm,[1] Shockley,[2] Bardeen,[3] and others[4–7] concerning the theoretical foundation of surface states. An infinite superlattice separates the free-electron continuum into allowed bands of extended states and forbidden bands as a result of the periodicity of the lattice. However, if this periodicity is broken by the addition of an interface, as in the case of a semi-infinite superlattice, then the existence of surface states localized at the interface becomes possible. Ohno *et al.*[8] experimentally observed Tamm surface states in these structures using a combination of photoluminescence, photoluminescence excitation, and photocurrent spectroscopies. They also performed numerical calculations on a nine-well $Al_{0.2}Ga_{0.8}As/GaAs$ superlattice as a function of interface potential and obtained excellent agreement with their experimental results, verifying the existence of localized surface states. Huang[9] did theoretical modeling of these surface states within the Kronig-Penney[10] (KP) model and also performed tunneling resonance calculations for a finite number of quantum wells. He also showed the possibility of mini-stop-gap mode for two coupled semi-infinite superlattices.[11]

In this work we investigate the surface states of a semi-infinite superlattice with a finite step discontinuity in the potential at the interface within the framework of the KP model with finite barrier heights and widths for the superlattice. This is distinct from Tamm, who used the δ function KP model in his classic work on surface states. The δ-function limit is inappropriate for typical III-V semiconductor superlattices grown by MBE or MOCVD. For well and barrier thicknesses greater than 20 Å, the KP model is a reasonable approximation to the band structure of superlattices. In this work we derive an exact equation for the surface-state energy for the arbitrary KP model which reduces to the Tamm surface state in the appropriate limit. In addition, we develop very accurate approximations for the surface-state energy and decay length which allows one to readily determine the conditions for the existence of the physically acceptable surface states. We apply these results in a detailed analysis of the surface states of two different semi-infinite superlattices as a function of varying barrier width and interface barrier height. As the barrier width decreases, the minibandwidths increase, and the surface state becomes unphysical. By the appropriate design of the semi-infinite superlattice, one can construct a surface state which has a large extension into the superlattice. These surface states may exhibit large Stark shifts and enhanced absorption, making them ideal candidates for optical modulators and detectors.

II. THEORY

In this paper we calculate the energy and condition for the existence of surface states for a semi-infinite superlattice with a finite step discontinuity within the KP model. The semi-infinite superlattice has a periodicity of length a, well width L_w, barrier width L_b, and barrier height V_0 as depicted in Fig. 1. At the interface there exists a step discontinuity in the potential, V_0'. V_0' can be greater or less than V_0. In this work we are interested in surface states whose wave functions are localized at the interface ($x=0$) and decay exponentially to zero on both sides of the interface. To find the surface states, we must solve the Schrödinger equation with the appropriate boundary conditions of continuity of the wave function and its

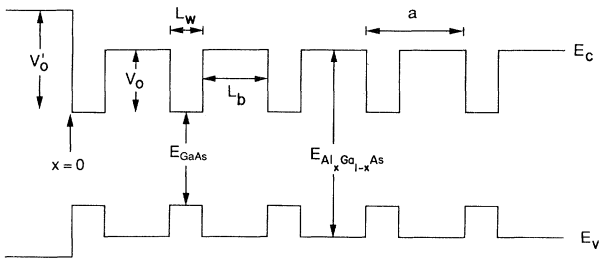

FIG. 1. Semi-infinite superlattice of quantum wells with periodicity a, well width L_w, barrier width L_b, and barrier height V_0. The interface at $x=0$ has a barrier height of V_0'.

derivative across every interface,

$$\left[-\frac{\hbar^2}{2m}\frac{d^2}{dx^2}+V(x)\right]\Psi(x)=\varepsilon\Psi(x)\ , \tag{1}$$

where m is the electron effective mass, $V(x)$ is the conduction-band profile, and ε the eigenenergy of the surface state. The potential energy for the conduction band is taken to be (see Fig. 1)

$$V(x)=\begin{cases}0 & \text{for } 0<x<L_w,\\ V_0 & \text{for } L_w<x<a\ ,\end{cases}$$

and is repeated periodically for $x>0$. For $x<0$,

$$V(x)=V_0'\ .$$

Solving Schrödinger's equation in each region for the wave function gives

$$\Psi_n(x)=\begin{cases}J_n e^{ikx}+L_n e^{-ikx} & \text{for } 0<x<L_w\ , \quad (2)\\ M_n e^{Kx}+N_n e^{-Kx} & \text{for } L_w<x<a\ , \quad (3)\end{cases}$$

where n labels the well-barrier unit cell starting from cell 0 at the interface and within the cell $\Psi_n(x)$ is defined for x measured from 0 at the origin of the unit cell to a at the end. For $x<0$ the wave function decays exponentially as

$$\Psi(x)=Fe^{K'x}\ , \tag{4}$$

where

$$\frac{\hbar^2k^2}{2m}=\varepsilon\ , \tag{5}$$

$$\frac{\hbar^2K^2}{2m}=V_0-\varepsilon\ , \tag{6}$$

$$\frac{\hbar^2K'^2}{2m}=V_0'-\varepsilon\ . \tag{7}$$

The effective electron mass for a $GaAs/Al_xGa_{1-x}As$ superlattice is 0.067 times the bare electron mass and is assumed to be the same in the GaAs and AlGaAs regions in the following analysis. This condition can easily be relaxed by applying the appropriate boundary condition of continuity of the inverse effective mass times the derivative of the wave function at each interface. Applying the boundary conditions at $x=a$ for cell n gives

$$J_n+L_n=M_{n-1}e^{Ka}+N_{n-1}e^{-Ka}\ , \tag{8}$$

$$ikJ_n-ikL_n=KM_{n-1}e^{Ka}-KN_{n-1}e^{-Ka} \tag{9}$$

and at $x=L_w$,

$$J_ne^{ikL_w}+L_ne^{-ikL_w}=M_ne^{KL_w}+N_ne^{-KL_w}\ , \tag{10}$$

$$ikJ_ne^{ikL_w}-ikL_ne^{-ikL_w}=KM_ne^{KL_w}-KN_ne^{-KL_w}\ . \tag{11}$$

If we assume a completely periodic superlattice (not semi-infinite), then the application of the Bloch condition ($\Psi_n=e^{in\bar{k}a}\Psi_0$) to Eqs. (8)–(11) results in four equations, the determinant of which equal to zero, results in the well-known equation for the allowed bands and forbidden gaps in the KP model,

$$\cos(\bar{k}a)=\cosh(KL_b)\cos(kL_w)+\frac{1}{2}\left[\frac{K}{k}-\frac{k}{K}\right]\sinh(KL_b)\sin(kL_w)\ , \tag{12}$$

where $\bar{k}$ is the Bloch wave vector defined over the first Brillouin zone ($-\pi/a<\bar{k}\le\pi/a$). In order to find the surface states of the semi-infinite superlattice, we make the ansatz of a decaying wave function away from the surface at $x=0$ into the superlattice ($\Psi_n=e^{-pna}\Psi_0$), which implies that

$$J_n=e^{-pna}J_0,\quad L_n=e^{-pna}L_0\ ,\qquad M_n=e^{-pna}M_0,\quad N_n=e^{-pna}N_0\ , \tag{13}$$

where p is the characteristic decay wave vector into the superlattice. Applying the boundary conditions at $x=0$ results in the additional equations

$$F=J_0+L_0\ , \tag{14}$$

$$K'F=ikJ_0-ikL_0\ . \tag{15}$$

Setting $L_0=cJ_0$, we solve the above equations:

$$K'=ik\frac{1-c}{1+c}\ . \tag{16}$$

In order to find c, we solve Eqs. (8)–(11) with the ansatz equation (13). After some amount of mathematics, we find the following equation for c:

$$c=\frac{e^{2ikL_w}[(ik+K)e^{pa}-(ik-K)e^{-2KL_b+pa}]-2Ke^{-KL_b+ikL_w}}{(ik-K)e^{pa}-(ik+K)e^{-2KL_b+pa}+2Ke^{-KL_b+ikL_w}}\ . \tag{17}$$

Substituting c into Eq. (16) and solving for $x=e^{pa}$,

$$x=\frac{1}{[\cosh(KL_b)\cos(kL_w)+(K'/K)\sinh(KL_b)\cos(kL_w)-(k/K)\sinh(KL_b)\sin(kL_w)+(K'/k)\cosh(KL_b)\sin(kL_w)]}\ . \tag{18}$$

Also, solving Eqs. (8)–(11) with the ansatz equation (13) (by setting the determinant of the set of equations equal to zero) gives

$$\cosh(pa)=\frac{1}{2}\left[x+\frac{1}{x}\right]=\cosh(KL_b)\cos(kL_w)+\frac{1}{2}\left[\frac{K}{k}-\frac{k}{K}\right]\sinh(kL_b)\sin(kL_w)\ . \tag{19}$$

Equation (19) is the analog of Eq. (12) for the allowed KP bands with $\bar{k}$ being replaced by ip for a decaying solution. Equations (18) and (19) completely specify the surface state and must be solved simultaneously. These equations can be solved numerically, albeit with a fair amount of computational effort. Here, after some amount of mathematics, we find that these two equations can be reduced to a simple equation for the surface-state eigenenergy:

$$\frac{K(k^2+K'^2)-K'(k^2+K^2)\tanh(KL_b)}{(K^2-K'^2)\tanh(KL_b)}=k\cot(kL_w)\ . \tag{20}$$

The above equation for the eigenenergy still must be solved numerically or graphically, but is readily solvable by most nonlinear equation-solver programs. It generalizes the Tamm surface-state solution to the case of an arbitrary superlattice. To our knowledge this is the first time that a simple equation for the surface states of the general KP model has been derived. After obtaining k from Eq. (20) and the corresponding surface-state energy from Eq. (5), the solution is substituted back into Eq. (18) in order to verify that it is a valid solution (decays exponentially). Only solutions with $x>1$ or $x<-1$ are physically acceptable. $x<-1$ corresponds to a decaying wave function that changes sign every lattice constant (that is, pa is equal to a real number plus $i\pi$).

Before proceeding further, we investigate Eq. (20) for the surface-state energy in the limit of the δ-function Kronig-Penney model. This limit is obtained by letting V_0 go to infinity and L_b go to zero in such a way that the product V_0L_b remains constant. After taking this limit, Eq. (20) reduces to the Tamm condition for the energy of the surface state:

$$ka\cot(ka)=\left[\frac{V_0'}{V_0}\right]\left[\frac{a}{L_b}\right]-\left[\frac{V_0'-\varepsilon}{E}\right]^{1/2}, \tag{21}$$

where E is a reduced energy defined to be $E=\hbar^2/2ma^2$. Applying the condition for a physically acceptable state, $x>1$ or $x<-1$, one can show that Eq. (18) within the δ-function limit results in the identical condition found by Tamm for an acceptable surface state:

$$\frac{mV_0L_b}{\hbar^2}>\left[\frac{2mV_0'}{\hbar^2}-k^2\right]^{1/2}. \tag{22}$$

By plotting Eq. (20) as a function of k, one finds that a surface state exists below the first energy band only if the left-hand side of Eq. (20) times L_w is less than unity since the limit of $kL_w\cot(kL_w)$ is 1 as k approaches zero and the left-hand side is a monotonically increasing function of k. In the δ-function limit, this leads to the condition, for an acceptable solution,

$$1>\left[\frac{V_0'}{V_0}\right]\left[\frac{a}{L_b}\right]-\left[\frac{V_0'}{E}\right]^{1/2}, \tag{23}$$

which is again in exact agreement to that found by Tamm for the δ-function KP model.

In the general case for the arbitrary KP model, one must solve Eq. (20) for the surface-state energy and substitute the answer into Eq. (18) for x in order to test for a physically acceptable solution. This is carried out in the analysis section below for two different superlattices. However, we now derive simple approximate equations for the surface-state energy and for x within a tight-binding-type approximation that allows us to determine easily the surface-state energy and its region of existence. This analysis is based on taking the large-KL_b limit. We begin by expanding Eq. (20) for the surface-state energy in the parameter $y=e^{-2KL_b}$. This leads to the following equation for the surface-state energy:

$$f(\varepsilon)=2g(\varepsilon)y=0\ , \tag{24}$$

where

$$f(\varepsilon)=(k^2-KK')\sin(kL_w)-k(K+K')\cos(kL_w)\ , \tag{25}$$

$$g(\varepsilon)=-\frac{K'(k^2+K^2)\sin(kL_w)+k(K^2-K'^2)\cos(kL_w)}{(K-K')}\ , \tag{26}$$

and we define

$$h(\varepsilon)=(k^2-K^2)\sin(kL_w)-2kK\cos(kL_w)\ . \tag{27}$$

We note that the equation for $f(\varepsilon)$ [Eq. (25)], set equal to zero (corresponding to infinite L_b), gives the eigenenergies for the states of an asymmetric quantum well with barriers V_0 and V_0' (the well at the interface; see Fig. 1). The function $h(\varepsilon)$ [which is simply $f(\varepsilon)$ with $K'=K$], when set equal to zero, gives the eigenenergies of a symmetric quantum well with barriers V_0 (this gives the centers of the allowed bands for the semi-infinite superlattice in this limit. Since y is assumed small in Eq. (24), it is natural to expand about the solution of $f(\varepsilon)$, which we denote as $\bar{\varepsilon}_0$, the eigenenergy of the isolated asymmetric quantum well. Expanding Eq. (24) about $\bar{\varepsilon}_0$, results in the following equation for ε:

$$\varepsilon\cong\bar{\varepsilon}_0+\left[2g(\varepsilon)e^{-2KL_b}\Big/\left[\frac{df(\varepsilon)}{d\varepsilon}\right]\right]_{\varepsilon=\bar{\varepsilon}_0}. \tag{28}$$

Similarly, we can expand Eq. (18) for x in y, then expand x about $\bar{\varepsilon}_0$, and use Eq. (24) to obtain

$$x=\left[\frac{e^{KL_b}(K-K')}{(k+KK'/k)\sin(kL_w)+(K-K')\cos(kL_w)}\right]_{\varepsilon=\bar{\varepsilon}_0}. \tag{29}$$

These approximate equations above for ε and x give very accurate results for most practical superlattices in the regions where physically acceptable solutions exist. This

will be discussed further in the next section. We now analyze Eq. (29) for solutions where $|x|>1$. We obtain the condition for a physically acceptable solution:

$$\left[2e^{-KL_b} < \left|\frac{K-K'}{K}\right| \left[\frac{V_0}{V_0'}\right]^{1/2}\right]_{\varepsilon=\bar{\varepsilon}_0} . \tag{30}$$

This is the generalization of the Tamm condition expressed by Eq. (22) to the arbitrary KP model. When Eq. (30) is an equality, this gives an accurate approximate solution for the parameters when the surface state no longer exists. Also, in analogy to the δ-function model, the solution to Eq. (20) for the surface state below the first miniband exists only when the left-hand side of the equation is less than unity (in the limit that k approaches 0) as discussed previously. In the small-y limit, this reduces to the following condition for a valid solution:

$$1-\frac{V_0'}{V_0} > \left[\frac{KL_w 4e^{-2KL_b}}{2+KL_w}\right]_{k=0} , \tag{31}$$

where $V_0'<V_0$. This is a generalization of the Tamm condition expressed in Eq. (23). In the superlattice structures that we have investigated, Eq. (30) is violated well before Eq. (31).

Before going into a detailed analysis of the above theoretical results to actual superlattices, we present a relatively simple model that contains much of the pertinent physics for the surface states of semiconductor superlattices. Although this model is not useful for accurate calculations, it does add insight to the previous results. This is the crystal-orbital method or tight-binding model.[6,7] In this model the physics of the semi-infinite superlattice is expressed in the following Hamiltonian, where ε_i is the energy of the quantum eigenstate at site i and t_{ij} is the overlap integral between the wave functions on site i and j, respectively:

$$H=\sum_i \varepsilon_i c_i^\dagger c_i + \sum_{i,j} t_{i,j} c_i^\dagger c_j , \tag{32}$$

where

$$\varepsilon_i = \begin{cases} \bar{\varepsilon}_0 & \text{for } i=0 , \\ \varepsilon_0 & \text{for } i\neq 0 , \end{cases}$$

$$t_{i,j}=t \quad \text{for all } j .$$

This is only an approximate Hamiltonian for our situation since it treats the overlap integral between wells 0 and 1 as identical to that between wells i and j. Although this assumption can be relaxed, it is not the situation here. However, it does treat the case where the quantum well at the interface has a different energy than the quantum wells in the superlattice, which, aside for the difference in the overlap integrals, is essentially the physics we do have here. The equation of motion in the Heisenberg picture is

$$\varepsilon c_i = \varepsilon_i c_i + \sum_j t_{i,j} c_j . \tag{33}$$

For a completely periodic superlattice and applying the Bloch condition ($c_j=e^{ijka}c_0$), it is easily shown that the tight-binding energy band is given by

$$\varepsilon=\varepsilon_0+2t\cos(\bar{k}a) , \tag{34}$$

where a is the periodicity of the superlattice. For the semi-infinite superlattice at site 0, we find

$$\varepsilon=\bar{\varepsilon}+te^{-pa} . \tag{35}$$

At any other site,

$$\varepsilon=\varepsilon_0+t(e^{pa}+e^{-pa}) . \tag{36}$$

From Eq. (35) we solve for x:

$$x=e^{pa}=\frac{t}{\varepsilon-\varepsilon_0} . \tag{37}$$

Substituting x into Eq. (36) and solving for the surface-state energy, we find

$$\varepsilon=\bar{\varepsilon}_0+\frac{t^2}{\bar{\varepsilon}_0-\varepsilon_0} . \tag{38}$$

Substituting this into Eq. (37) gives, for x,

$$x=\frac{\bar{\varepsilon}_0-\varepsilon_0}{t} . \tag{39}$$

The condition that $x>1$ or $x<-1$ leads to

$$|\bar{\varepsilon}_0-\varepsilon_0|>|t| . \tag{40}$$

This condition states that the difference in energy between the quantum-well energies ε_0, for the states in the superlattice, and $\bar{\varepsilon}_0$ for the quantum well at site 0 must be greater than one-quarter of the bandwidth in order to have a well-defined decaying surface state [from Eq. (34) the bandwidth is $4t$]. Basically, this defines the condition where the surface-state energy intersects the extended Bloch states of the superlattice and ceases to exist. Equations (38)–(40) provide a qualitative answer to the energy and condition for the existence of surface states. The essential physics of surface-state formation relevant to III-V semiconductor superlattices is embodied in this simple tight-binding model. However, in most cases for direct experimental comparisons, one would want to rely on either the exact solution given by Eqs. (18) and (20) or the approximate but accurate equations given by Eqs. (28) and (29). In the next section, we apply these results to two different superlattices.

III. ANALYSIS AND RESULTS

In this section we apply the above theoretical results for the surface states of a semi-infinite superlattice to two different $GaAsAl_xGa_{1-x}As$ superlattices. In both superlattices the barrier height V_0 is fixed at 240 meV appropriate to an x concentration of approximately 0.3. For the first superlattice, the quantum-well width is fixed at 40 Å, but the barrier width is allowed to vary. The second superlattice we consider has a quantum-well width fixed at 80 Å. For the 40-Å quantum well, there is only one confined state in the quantum well and, consequently, only one energy band below V_0, whereas for the 80-Å quantum well there are two confined energy states

and two energy bands. The surface state is calculated numerically from Eq. (20) and also from the approximate relation [Eq. (28)]. Likewise, x is calculated from the exact relation [Eq. (18)] and from the approximate equation [Eq. (29)]. The condition for the validity of a surface state [Eq. (30)] is also investigated.

In Fig. 2 we plot the surface-state energy (solid line) as a function of barrier width for the superlattice with $L_w = 40$ Å and $V_0 = 240$ meV from the solution of the exact equation (20). In Fig. 2(a) the interface barrier is 180 meV (lower than V_0) and in Fig. 2(b) is 300 meV (higher than V_0). For large barrier width, the surface-state energy approaches 95.86 meV for the 180-meV barrier and 109.44 meV for the 300-meV barrier. These are just the eigenenergies for an asymmetric quantum well determined by setting Eq. (25) to zero. The dotted lines in the figure depict the edges of the KP band for the infinite superlattice. The center of the band for large L_b is given by the zero of Eq. (27) and is 103.81 meV. For the lower (higher) barrier case (Fig. 2(a) [2(b)]), as the barrier width is reduced, the surface state interacts with the extended states of the superlattice and its energy is pushed downward (upward) as the band becomes wider. Eventually, the surface-state energy intersects the superlattice band and is no longer a physically acceptable solution. This is shown in Figs. 3(a) and 3(b), where we plot x versus the barrier width derived from the exact equation (18) for the superlattices of Figs. 2(a) and 2(b), respectively. For large L_b, x is large, implying a rapidly decaying wave function. In Fig. 3(b), corresponding to the higher barrier, x is negative and the wave function changes sign from each adjacent quantum well. As L_b gets smaller, x decays in magnitude for both Figs. 3(a) and 3(b), eventually approaching a magnitude of unity. For an absolute value of x less than unity, the solution is unphysical. For the 180-meV interface, the critical barrier width below which the solution is unphysical is 40.27 Å; for the 300-meV barrier the critical L_b is 49.74 Å. As we get close to the critical barrier thickness, x is close to unity and the wave function extends a substantial distance into the interface. In particular, the number of lattice spacings over which the surface state extends into the superlattice is $n = 1/\ln(x)$ (this is the condition when $e^{-pna} = 0.368$). For $x = 1.2$ the surface state extends over 5.5 lattice spacings from the interface; for $x = 1.1$ it extends 10.5 lattice spacings. In both Figs. 2 and 3, the solid dots in the figures are the results of the approximate equations (28) and (29), which are seen to give extremely accurate results. We have also calculated the surface-state energies and the corresponding x values by using the qualitative equations derived from the tight-binding approximation [Eqs. (38) and (39)]. In this case we take the bandwidth ($4t$) to be equal to that derived from the KP model. These equations provide reasonable results for energies much less than V_0 and for bandwidths that are not too wide. For example, for $L_b = 50$ Å, we obtain a surface-state energy of 92.34 meV and x value of 1.50 for $V_0' = 180$ and 114.40 meV and -1.06 for $V_0' = 300$ meV. The exact values are 93.29 meV and 1.67 for $V_0' = 180$ meV and 115.55 meV and -1.01 for $V_0' = 300$ meV.

Using Eq. (30) for the condition for a valid solution

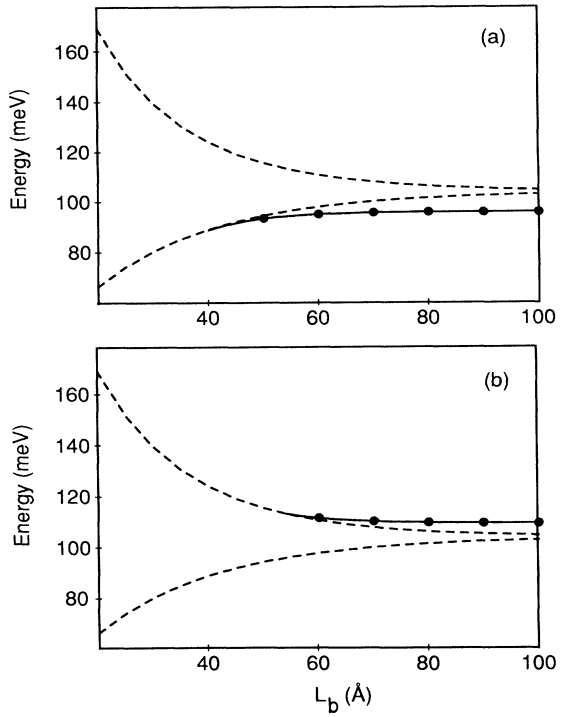

FIG. 2. (a) Plot of the surface-state energy vs barrier width for $L_w = 40$ Å, $V_0 = 240$ meV, and $V_0' = 180$ meV and (b) for $V_0' = 300$ meV.

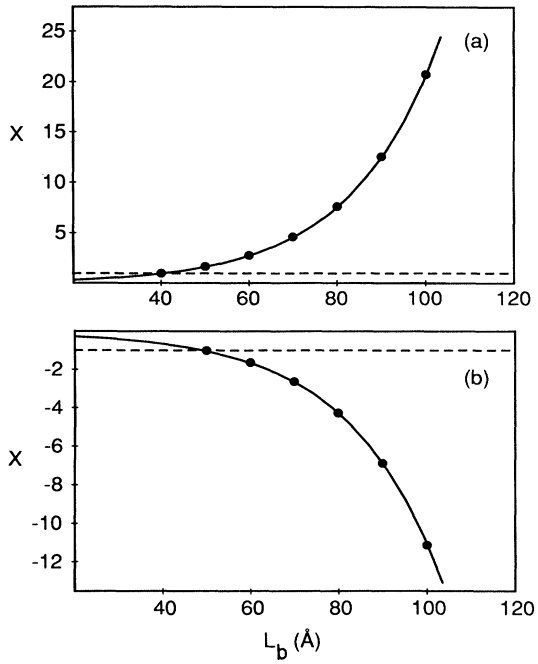

FIG. 3. (a) Plot of x for the superlattice of Fig. 2(a) and (b) for Fig. 2(b).

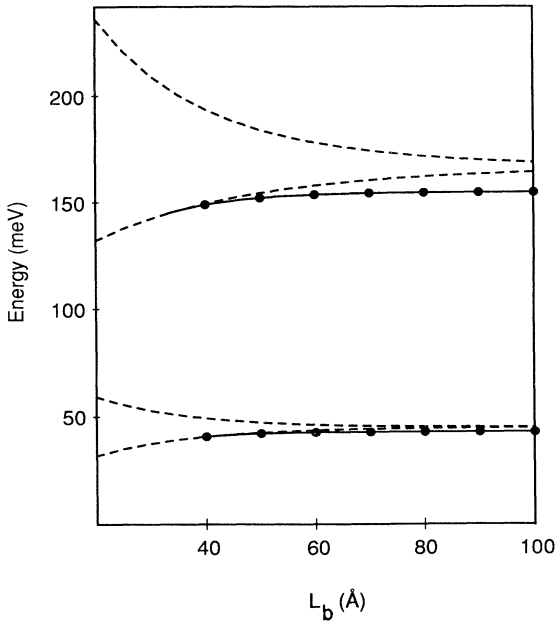

FIG. 4. Plot of the surface-state energy vs barrier width for $L_w = 80$ Å, $V_0 = 240$ meV, and $V_0' = 180$ meV.

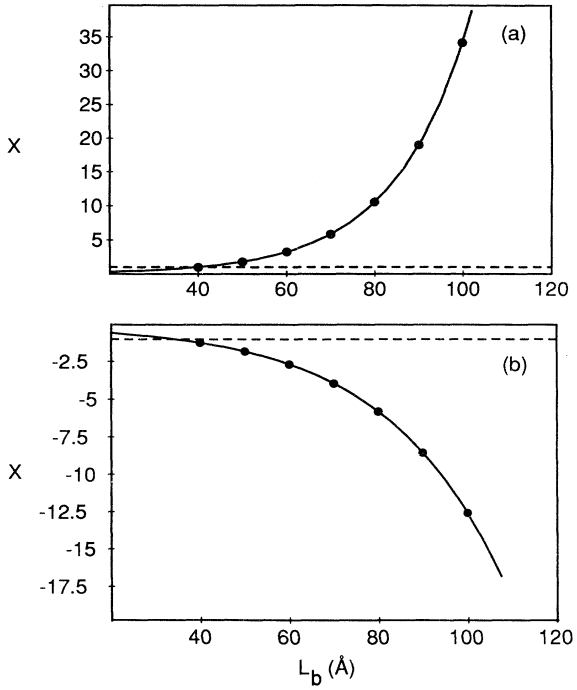

FIG. 5. (a) Plot of x for the lower-band surface state of Fig. 4 and (b) for the upper-band surface state.

($|x| > 1$), we find that surface states exist for $L_b > 39.66$ Å (for the lower barrier and $L_b > 49.64$ Å (for the higher barrier), in excellent agreement with the above exact results. From the condition Eq. (31), we find that a surface state exists below the first miniband for $V_0' < 238.49$ meV for $L_b = 40$ Å. However, at this value of V_0', we find from Eq. (30) that there is no solution below $L_b = 118.17$ Å. Thus the first condition is violated well before the second, and for the superlattices considered here we can ignore the second condition. A final point concerns the existence of surface states for energies greater than V_0. We find that if V_0' is larger than V_0, then surface states can exist above V_0. In particular, for $V_0' = 600$ meV and $L_b = 40$ Å, we find a surface state with energy 465.58 meV and $x = 1.1$. In this case the second miniband is in the continuum above V_0 and extends from 273.99 to 461.83 meV. The surface state is just above the second miniband. This result is obtained from the exact equation (20) for the surface-state energy by the substitution of $K \rightarrow iK$ for states in the superlattice continuum (above $V_0 = 240$ meV).

In Figs. 4–7 we plot the results for a superlattice with a well width of 80 Å. For isolated quantum wells of the semi-infinite structure, there are two bound-energy states at 44.98 and 166.18 meV. As the barrier width decreases, the wells become coupled and two minibands are formed (for energies less than V_0; there are also bands in the continuum above V_0). The results for the surface-state energies depicted in Fig. 4 are for an interface barrier of 180 meV and in Fig. 6 for 300 meV. For the 180-meV barrier, we find two surface states, one below each band. The isolated quantum well at the interface has two eigenstates at 42.94 and 154.66 meV. As in the previous figures, the solid lines are for the exact calculation, the dotted lines show the superlattice bands, and the dots are from the approximate equations. The critical barrier widths from the exact equations are $L_b = 40.87$ Å (lower band) and $L_b = 34.32$ Å (upper band) with the approximate results from Eq. (30) giving $L_b = 39.90$ and 34.56 Å, respectively. Excellent agreement is obtained between the exact and approximate equations. We also see that

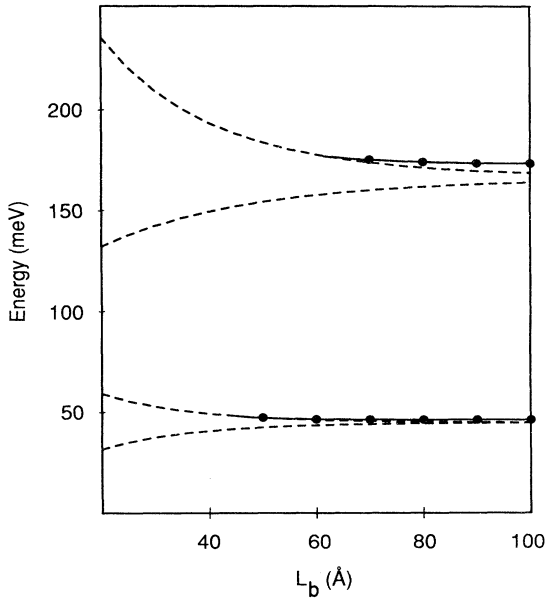

FIG. 6. Plot of the surface-state energy vs barrier width for $L_w = 80$ Å, $V_0 = 240$ meV, and $V_0' = 300$ meV.

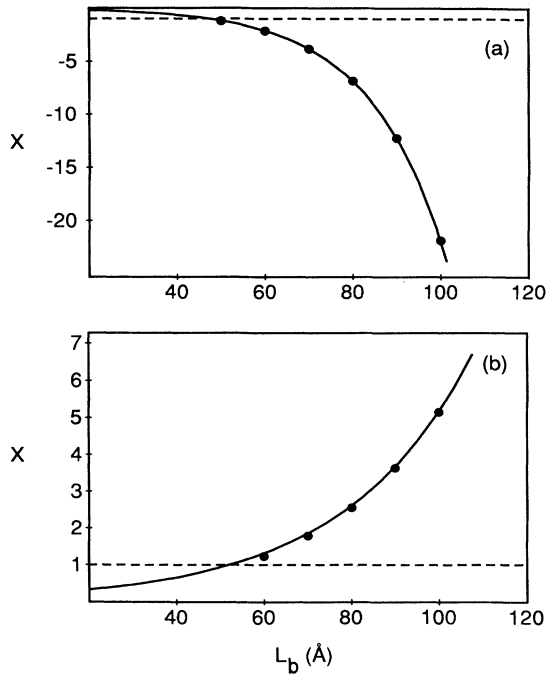

FIG. 7. (a) Plot of x for the lower-band surface state of Fig. 6 and (b) for the upper-band surface state.

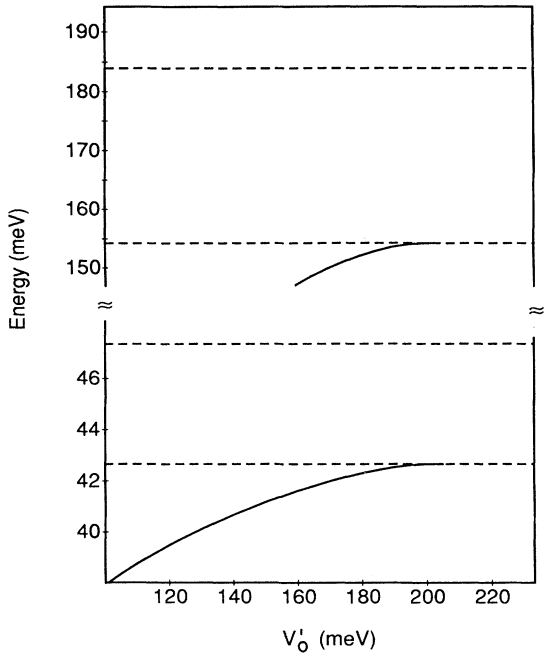

FIG. 8. Plot of the surface-state energy for $L_w=80$ Å and $L_b=50$ Å as a function of interface barrier height V_0' for $V_0'<240$ meV.

there is a region of barrier widths between 34 and 40 Å in which only the upper-band surface state is allowed. Results for x are given in Fig. 5(a) (lower band) and Fig. 5(b) (upper band). Note that the surface state associated with the upper band has negative x.

In Fig. 6 we plot the surface-state energy for an interface barrier of 300 meV. Now the surface states occur above the bands. The critical barrier widths are $L_b=46.37$ Å (lower band) and $L_b=54.44$ Å (upper band), in agreement with the approximate results $L_b=47.02$ and 51.97 Å, respectively. For the higher interface barrier, there is a region of barrier widths, between 40 and 54 Å, in which only the lower-band surface state exists. In Figs. 7(a) and 7(b) we plot x for the lower and upper bands, respectively. Note that the surface state associated with the lower band now has negative x and that with the upper band has a positive x. This is true in general. There is a slight inaccuracy in energy and x for the upper surface state for the 300-meV barrier superlattice since $e^{-KL_b}\approx 0.19$ at $L_b\approx 50$ Å, which implies that y is no longer small. The approximate results based on y being small become less accurate as the energy gets closer to V_0. For lower energies the approximate results are extremely accurate.

In Figs. 8–11 we investigate the superlattice with fixed barrier width $L_b=50$ Å, but as a function of varying interface barrier height V_0'. The dotted lines in Figs. 8 and 10 are the edges of the superlattice bands, and the solid lines are the exact results for the surface-state energies. In Fig. 8, for $V_0'<V_0$, we find that the surface states intersect the bands at $V_0'=202.37$ meV for the lower band and for $V_0'=202.27$ meV for the upper band. The approximate equation (30) gives $V_0'=203.44$ and 200.82 meV, respectively. For V_0' larger than these values, the surface states become unphysical. We also plot, in Figs. 9(a) and 9(b), x for the surface states associated with the

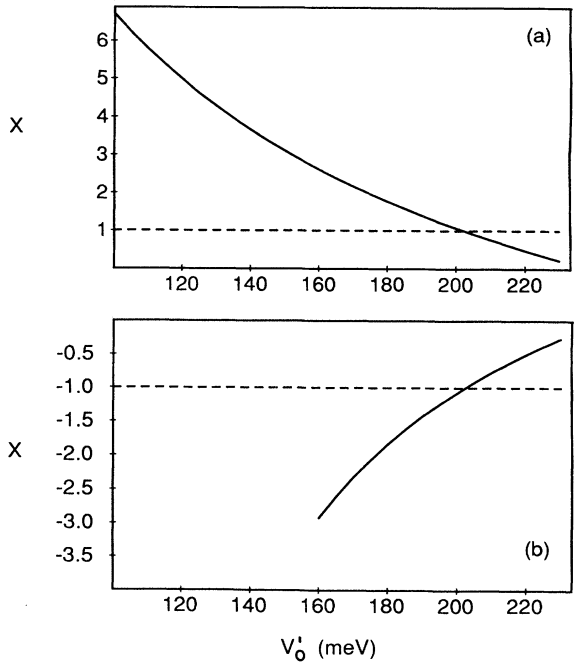

FIG. 9. (a) Plot of x for the lower-band surface state of Fig. 8 and (b) for the upper-band surface state.

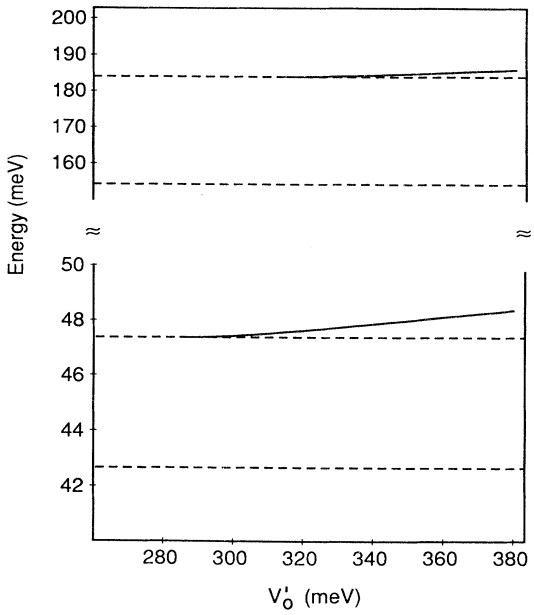

FIG. 10. Plot of the surface-state energy for $L_w = 80$ Å and $L_b = 50$ Å as a function of interface barrier height V_0' for $V_0' > 240$ meV.

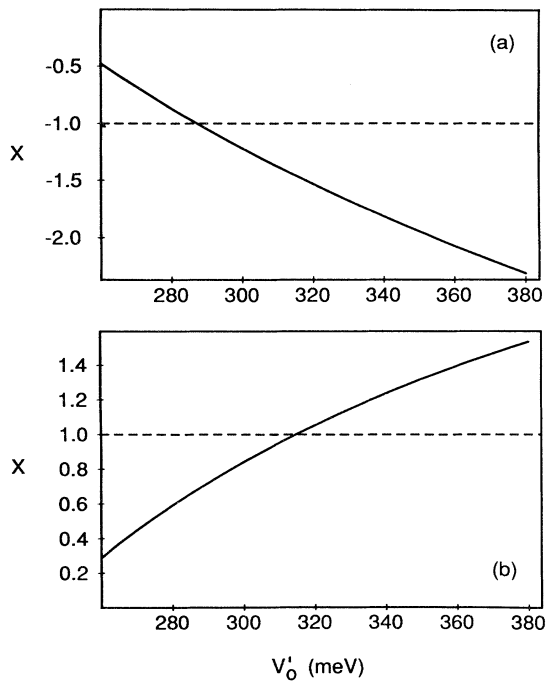

FIG. 11. (a) Plot of x for the lower-band surface state of Fig. 10 and (b) for the upper-band surface state.

lower and upper bands, respectively. Figures 10 and 11 depict the same calculation, but for V_0' higher than V_0. Here the surface states intersect the band and become unphysical at $V_0' = 287.21$ meV for the lower band and $V_0' = 314.70$ meV for the upper band with the approximate results $V_0' = 288.93$ and 305.60 meV. For V_0' smaller than these values, the states become unphysical. Again, the approximate equations give accurate results except for the surface state of the higher-energy band of Fig. 10 where e^{-2KL_b} is no longer small.

IV. CONCLUSION

In conclusion, we have derived an explicit formula for the surface states of a semi-infinite superlattice within the KP model. In addition, we have investigated the conditions where valid surface states exist. Approximate equations were also derived, which give rather accurate results in most situations. A detailed analysis of two superlattices with different quantum-well widths as a function of barrier width was performed. We showed that there are regions in parameter space (L_w, L_b, V_0, V_0') where surface states cannot exist. We also showed that the semi-infinite superlattice can be designed so that x is close to one corresponding to a large extension of the surface-state wave function into the superlattice. Semiconductor superlattices structures grown by MBE and MOCVD should prove extremely useful for surface-state investigations.

ACKNOWLEDGMENT

This work was supported by The Aerospace Sponsored Research Program.

[1] I. Tamm, Phys. Z. Sowjet Union **1**, 733 (1932).
[2] W. Shockley, Phys. Rev. **56**, 317 (1939).
[3] J. Bardeen, Phys. Rev. **71**, 717 (1947).
[4] A. W. Maue, Z. Phys. **94**, 717 (1935).
[5] E. T. Goodwin, Proc. Cambridge Philos. Soc. **35**, 205 (1939); **35**, 221 (1939); **35**, 232 (1939).
[6] S. G. Davison and J. D. Levine, *Surface States,* Vol. 25 of *Solid State Physics,* edited by H. Ehrenreich and D. Turnbill (Academic, New York, 1970), p. 1.
[7] J. Koutecky, Adv. Chem. Phys. **9**, 85 (1965).
[8] H. Ohno, E. E. Mendez, J. A. Brum, J. M. Hong, F. Agullo-Rueda, L. L. Chang, and L. Esaki, Phys. Rev. Lett. **64**, 2555 (1990).
[9] F. Y. Huang, Appl. Phys. **57**, 1669 (1990).
[10] R. de L. Kronig and W. G. Penney, Proc. Soc. London Sect. A **130**, 499 (1931).
[11] F. Y. Huang, Appl. Phys. **57**, 2199 (1990).